



Published in final edited form as:

*Gastroenterology*. 2020 March ; 158(4): 971–984.e10. doi:10.1053/j.gastro.2019.11.013.

## Prostaglandin E<sub>2</sub> Induces MIR675-5p to Promote Colorectal Tumor Metastasis via Modulation of p53 Expression

Bo Cen<sup>1, #</sup>, Jessica D. Lang<sup>2, #</sup>, Yuchen Du<sup>3</sup>, Jie Wei<sup>1</sup>, Ying Xiong<sup>1</sup>, Norma Bradley<sup>1</sup>, Dingzhi Wang<sup>1</sup>, Raymond N. DuBois<sup>1, 4, \*</sup>

<sup>1</sup>Department of Biochemistry and Molecular Biology, Medical University of South Carolina, Charleston, Charleston, SC 29425.

<sup>2</sup>Biodesign Institute of Arizona State University, Tempe, AZ85287, and Integrated Cancer Genomics Division, Translational Genomics Research Institute (TGen), Phoenix, AZ 85004.

<sup>3</sup>Biodesign Institute of Arizona State University, Tempe, AZ85287 (current address: Department of Pediatrics-Oncology, Baylor College of Medicine, Houston, TX77030)

<sup>4</sup>Department of Research and Division of Gastroenterology, Mayo Clinic, Scottsdale, AZ 85259

### Abstract

**BACKGROUND & AIMS**—Prostaglandin E<sub>2</sub> (PGE<sub>2</sub>) promotes colorectal tumor formation and progression by unknown mechanisms. We sought to identify microRNAs (miRNAs) that might mediate the effects of PGE<sub>2</sub> on colorectal cancer (CRC) development.

**METHODS**—We incubated LS174T colorectal cancer cells with PGE<sub>2</sub> or without (control) and used miRNA-seq technology to compare expression patterns of miRNAs. We knocked down levels of specific miRNAs or proteins in cells using small interfering RNAs or genome editing. Cells were analyzed by immunoblot, quantitative PCR, chromosome immunoprecipitation, cell invasion, and luciferase reporter assays; we measured gene expression, binding activity, cell migration and invasion, and transcriptional activity of transcription factors. NSG mice were given injections of LS174T cells and growth of primary tumors and numbers of liver and lung metastases were quantified and analyzed by histology. We used public databases to identify correlations in gene expression pattern with patient outcomes.

**RESULTS**—We identified miRNA 675-5p (MIR675-5p) as the miRNA most highly upregulated by incubation of colorectal cancer cells with PGE<sub>2</sub>. PGE<sub>2</sub> increased expression of MIR675-5p by activating expression of Myc, via activation of AKT, NF-κB, and β-catenin. β-catenin PGE<sub>2</sub>

\* **Correspondence to:** Raymond N. DuBois, MD, Ph.D., 601 Clinical Science Building, 96 Jonathan Lucas Street, Suite 601, Charleston, SC 29425. Tel: 843-792-2842 and Fax: 843-792-2967, duboisrn@muscc.edu.

#These authors contribute equally.

**Author contributions:** R.N.D. supervised the entire study. B.C. and D.W. designed the experiments. B.C., J.D.L., Y.D., J.W., Y.X., and N.B. performed experiments. J.D.L. performed bioinformatics analysis. B.C. and J.D.L. wrote the manuscript. D.W. and R.N.D. edited the manuscript.

**Disclosures:** The authors declare no competing interests.

**Publisher's Disclaimer:** This is a PDF file of an unedited manuscript that has been accepted for publication. As a service to our customers we are providing this early version of the manuscript. The manuscript will undergo copyediting, typesetting, and review of the resulting proof before it is published in its final form. Please note that during the production process errors may be discovered which could affect the content, and all legal disclaimers that apply to the journal pertain.

increased the invasive activities of cultured CRC cells. LS174T cells incubated with PGE<sub>2</sub> formed more liver and lung metastases in mice than control LS174T cells. We identified a 3'UTR in the *TP53* mRNA that bound MIR675-5p; binding resulted in loss of the p53 protein. Expression of MIR675-5p or its precursor RNA, H19, correlated with expression of cyclooxygenase-1 and cyclooxygenase-2 and shorter survival times of patients with CRC.

**CONCLUSIONS**—We found incubation of CRC cells with PGE<sub>2</sub> to increase their invasive activity and ability to form liver and lung metastases in mice. PGE<sub>2</sub> downregulates expression of p53 by increasing expression of MIR675-5p, which binds to and prevents translation of *TP53* mRNA. These findings provide insight into the mechanisms by which PGE<sub>2</sub> promotes tumor development and progression. Strategies to target the PGE<sub>2</sub> might be developed for treatment of CRC.

**BACKGROUND AND CONTEXT**—Prostaglandin E<sub>2</sub> (PGE<sub>2</sub>) promotes colorectal tumor formation and progression by unknown mechanisms.

**NEW FINDINGS**—We found incubation of CRC cells with PGE<sub>2</sub> to increase their invasive activity and ability to form liver and lung metastases in mice. PGE<sub>2</sub> downregulates expression of p53 by increasing expression of MIR675-5p, which binds to *TP53* mRNA and prevents its translation.

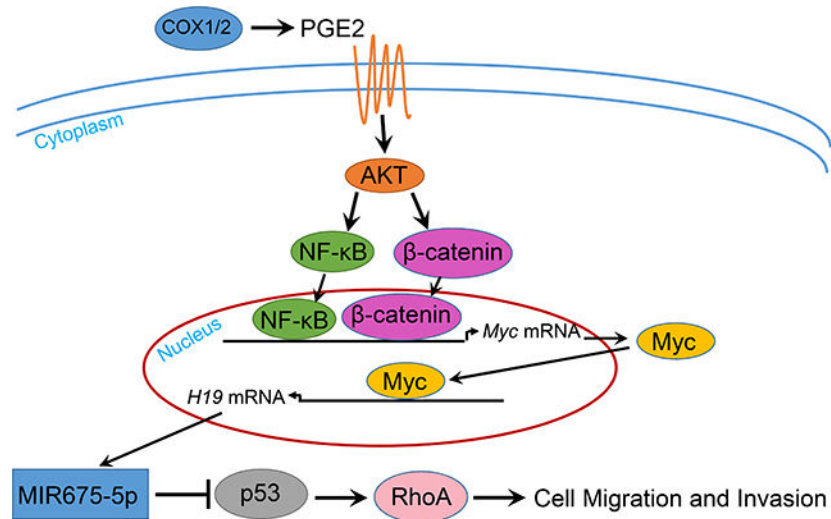
**LIMITATIONS**—These studies were performed in cell lines and mice. Studies in humans are needed.

**IMPACT**—These findings provide insight into the mechanisms by which PGE<sub>2</sub> promotes tumor development and progression. Strategies to target the PGE<sub>2</sub> might be developed for treatment of CRC.

## LAY SUMMARY

The pro-inflammatory prostaglandin E<sub>2</sub> induces MIR675-5p by induction of Myc expression via activation of AKT, NF- $\kappa$ B and  $\beta$ -catenin. MIR675-5p targets p53 to enhance RhoA activity to promote colorectal cancer metastasis.

## Graphical Abstract



## Keywords

gene regulation; tumor suppressor; post-transcriptional modification; inflammation

## Introduction

Prostaglandins (PGs) are bioactive lipids that impact normal development, tissue homeostasis, inflammation, and cancer progression<sup>1</sup>. PGs are produced from arachidonic acid by action of prostaglandin-endoperoxide synthases 1 (PTGS1) and/or prostaglandin-endoperoxide synthases 2 (PTGS2), also referred to as cyclooxygenase 1 (COX-1) and cyclooxygenase 2 (COX-2). COX-1 helps maintain gastric epithelial cytoprotection and homeostasis<sup>2</sup>. COX-2, induced by inflammatory stimuli, hormones and growth factors, is elevated in inflammatory and proliferative diseases, such as cancer<sup>2</sup>. COX-2 levels are increased in multiple cancer types and are associated with decreased survival among cancer patients<sup>3-5</sup>. The activity of COX-1/2 can be inhibited by nonsteroidal anti-inflammatory drugs (NSAIDs) which are known to reduce the risk of CRC<sup>6</sup>. PGE<sub>2</sub> is a commonly studied PG and the most abundant one found in various types of human malignancies and higher levels correlate with a poor prognosis<sup>7-9</sup>. A urinary PGE<sub>2</sub> metabolite (PGE-M) levels are associated with an increased risk of multiple human cancers<sup>10</sup>. PGE<sub>2</sub> exerts its effects by binding to cell surface EP receptors that belong to the family of G protein-coupled receptors. Each EP receptor activates distinct downstream signaling pathways that transduce a particular biologic effect. PGE<sub>2</sub> has been shown to promote tumor epithelial cell proliferation, survival, and migration/invasion via multiple signaling pathways<sup>1</sup>. However, all of the mechanisms by which PGE<sub>2</sub> accelerates cancer formation, progression, and metastasis in complex living systems have not been fully elucidated.

A growing number of reports suggest that the H19 long intergenic noncoding RNA (lincRNA) expression is linked to carcinogenesis<sup>11</sup>. H19 was found to be the precursor of two distinct microRNAs (miRNAs), MIR675-5p and MIR675-3p<sup>12</sup>. It has been suggested that these miRNAs partially confer functionality of H19<sup>12, 13</sup>. The levels of MIR675 (by

convention, MIR675 refers to the MIR675-5p.) are significantly increased in several cancer tissues such as glioma<sup>14</sup>, gastric cancer<sup>15</sup>, CRC<sup>16</sup>, non-small cell lung cancer<sup>17</sup>, hepatocellular cancer<sup>18</sup>, and breast cancer<sup>19</sup>. It is not clear how MIR675 is regulated in cancers, and like H19, the role of MIR675 in cancer development and metastasis was observed in separate studies<sup>17, 19–22</sup>. Here, we investigate the role of MIR675-5p in PGE<sub>2</sub>-induced CRC invasion and metastasis.

## Materials and Methods

### MiRNA

Total RNA from cells was extracted using the miRNeasy Mini Kit (Qiagen) and reverse transcribed by the miRCURY™ LNA™ Universal RT microRNA PCR Universal cDNA Synthesis Kit II (Exiqon/Qiagen). Expression of miRNAs was examined by quantitative polymerase chain reaction (qPCR) using iQ SYBR Green Supermix (BioRad) and miRCURY microRNA assays (Exiqon/Qiagen) on a QuantStudio 7 Flex Real-Time PCR System (Thermo Fisher Scientific). Human SNORD44 was measured as a control.

### Clustered regularly interspaced short palindromic repeats(CRISPR)/Cas9 system

To generate CRISPR/Cas9 plasmids targeting MIR675, p53, AKT1, AKT2, and Myc, primers of single-guide RNAs were synthesized at Integrated DNA Technologies, annealed, ligated into LentiCRISPRv2 (Addgene #52961) and transduced to cells by lentivirus using Lenti-X packaging single shots (VSV-G, Clontech #631275) and 293T cells. Transduced cells were selected with puromycin and pooled. The targeted sequences are listed in the supplementary Materials and Methods.

### Animal Experiments

Animal studies were performed in compliance with institutional guidelines under an IACUC approved protocol at MUSC or Arizona State University. NOD-scidIL-2Rg<sup>-/-</sup> (NSG) mice were obtained from Jackson Laboratory (Bar Harbor, ME) and bred in-house. For the orthotopic mouse model, 25,000 cells derived from LS174T cells were injected into the cecal wall of male NSG mice at the age of 8 weeks. Four days later, PGE<sub>2</sub> (Cayman Chemical #14010) or vehicle were given to mice through intraperitoneal injection at 300 µg/mouse/day. PGE<sub>2</sub> was dissolved in 100% ethanol and diluted to desired concentration with PBS immediately before the injection. The mice were sacrificed at 8 weeks for experiment with p53 overexpression and at 6 weeks for experiment with p53 CRISPR depletion after the start of the treatment. Metastatic nodules on livers were visually inspected and counted. Metastatic nodules on lungs were revealed by India ink staining and counted. Primary cecal tumors were isolated and weighted. Haematoxylin and eosin stain was performed on sectioned liver and lung to confirm tumor histology.

### Statistical Analysis

The results of quantitative studies are reported as mean ± SD or Mean ± SEM (for animal experiments). The SEM/SD was calculated based on the number of independent experiments. Differences were analyzed by two-sided Student's t test. *P* values of < .05 were regarded as significant.

Procedures of several methods, including *in vitro* cell invasion assay, luciferase reporter assays, human CRC patient specimens and tissue microarray, miR-Seq analysis, cell culture and transfection, immunoblotting, siRNAs, RhoA pull-down activation assay, RNA-ChIP and qPCR, p53 pathway RT<sup>2</sup> Profiler PCR array, chromatin immunoprecipitation, and public data mining, are available in the supplementary Materials and Methods.

## Results

### PGE<sub>2</sub> induces MIR675-5p expression in CRC cells

To identify miRNAs that mediate effects of PGE<sub>2</sub> on CRC cells, we conducted a miRNA-Seq experiment on LS174T cells treated with PGE<sub>2</sub>. Next generation sequencing data analysis identified a total of 403 miRNAs among which 56 miRNAs (FDR < 0.4) were responsive to PGE<sub>2</sub> at all three time points (Figure 1A and Supplementary Table 1). We confirmed changes of some of the top candidates by qPCR assays (Supplementary Figure 1). The most strongly induced miRNA was MIR675-5p. The induction of MIR675-5p was obvious even when the PGE<sub>2</sub> concentrations was as low as 0.01 μM (Figure 1B). Dose-dependent expression of MIR675-3p and lincRNA H19 were also observed (Figure 1B). The induction of MIR675-5p and H19 was reproducible in multiple CRC cell lines treated with 1 μM PGE<sub>2</sub> except for HCT116 which required higher doses of PGE<sub>2</sub> (Figure 1C). More importantly, treatment of primary CRC cells isolated from CRC patient specimens with PGE<sub>2</sub> robustly induced MIR675-5p expression (Figure 1D). We analyzed public databases and found that expression of MIR675-5p was significantly upregulated in the CRC tissues compared with normal tissues (Figure 1E). This finding was confirmed by evaluation of samples from a different cohort of patients in a CRC tissue microarray (Figure 1F). Similarly, we observed upregulation of H19 in the CRC tissues when compared with normal tissues in two separate public databases (Figure 1G). As expected, H19 expression strongly correlated with MIR675-5p expression in CRC patient samples (Supplementary Figure 2).

### NF-κB and β-catenin converge on the *Myc* promoter to control H19/MIR675-5p expression

PGE<sub>2</sub> activated AKT by inducing phosphorylation of AKT in LS174T and SW48 cells (Supplementary Figure 3 A and B). PGE<sub>2</sub> also activated the NF-κB by inducing phosphorylation of NF-κB and degradation of I-KBα via reducing its half-life (Supplementary Figure 3 A, B and C). Furthermore, PGE<sub>2</sub> activated a NF-κB responsive element (Supplementary Figure 3D, left panel) and caused nuclear translocation of NF-κB (Supplementary Figure 3E). Meanwhile, PGE<sub>2</sub> also activated the β-catenin by inducing increased levels of active β-catenin (non-phosphorylation on Ser33/Ser37Thr41) (Supplementary Figure 3 A and B). PGE<sub>2</sub> also stimulated the activity of a TOPflash (TCF reporter) (Supplementary Figure 3D, right panel) and induced nuclear translocation of β-catenin (Supplementary Figure 3F). To determine whether these signaling molecules are involved in PGE<sub>2</sub> induction of MIR675-5p, CRISPR/Cas9 and siRNA technologies were deployed. CRISPR depletion of AKT1 or AKT2 inhibited PGE<sub>2</sub>-induced expression of MIR675-5p (Figure 2A) and H19 (Figure S3G, left panel). Similarly, knockdown of NF-κB (Figure 2C) or β-catenin (Figure 2D) with siRNAs attenuated the effect of PGE<sub>2</sub> on induction of MIR675-5p and H19 (Figs. 2A and Supplementary 3G).

To further determine how these signaling molecules regulate the expression of H19 and MIR675-5p, we found that depletion of AKT1, AKT2, NF- $\kappa$ B, or  $\beta$ -catenin, or treatment with their inhibitors blocked PGE<sub>2</sub> induction of Myc expression at both protein (Figure 2 B–D and Supplementary Figure 3 H and I) and mRNA levels (Figure 2E). These results demonstrate that Myc is a downstream target of these molecules. Moreover, the AKT inhibitor MK2206, I- $\kappa$ B inhibitor BAY11-7085, or a  $\beta$ -catenin inhibitor FH535 blocked *Myc* promoter activity induced by PGE<sub>2</sub> in the luciferase reporter assays (Figure 2F). Additionally, analysis of ChIP assays showed that PGE<sub>2</sub> induced the binding of  $\beta$ -catenin and NF- $\kappa$ B to the promoter of the *Myc* gene (Figure 2G). In agreement with previous findings<sup>23</sup>, our ChIP assays showed that PGE<sub>2</sub> increased the binding of Myc to the promoter of the *H19* gene, which can be suppressed by the inhibitors of AKT, I- $\kappa$ B, or  $\beta$ -catenin (Figure 2H). Depletion of Myc inhibited PGE<sub>2</sub> induction of MIR675-5p (Figure 2I) and H19 (Supplementary Figure 3J), demonstrating that Myc is required for PGE<sub>2</sub>-induced expression of MIR675-5p and H19.

We further examined whether activation of AKT activates NF- $\kappa$ B. MK2206 blocked PGE<sub>2</sub>-induced degradation of I- $\kappa$ B $\alpha$  and phosphorylation of NF- $\kappa$ B (Figure 2J), suggesting that activation of AKT leads to activation of NF- $\kappa$ B pathway. In support of this notion, MK2206 inhibited the phosphorylation of Thr23 on IKK $\alpha$  (Figure 2K). Phosphorylation of Thr23 on IKK $\alpha$  by AKT is a prerequisite for the phosphorylation of NF- $\kappa$ B at Ser534 by IKK $\alpha$ <sup>24</sup>. Moreover, knockdown of IKK $\alpha$  inhibited PGE<sub>2</sub>-induced degradation of I- $\kappa$ B $\alpha$  and phosphorylation of NF- $\kappa$ B (Supplementary Figure 3K).

A previous study suggested that PGE<sub>2</sub> induces  $\beta$ -catenin stabilization/activation partially through AKT-GSK-3 $\beta$  cascade<sup>25</sup>. Indeed, we found that treatment of cells with PGE<sub>2</sub> led to the rapid phosphorylation of GSK-3 $\beta$  on serine 9, which requires AKT activity as it was blocked by AKT or PI3K inhibitors (Supplementary Figure 3H). It does not appear that PGE<sub>2</sub> treatment increases receptor-mediated WNT signaling as we did not detect increased phosphorylation of LRP6 co-receptor (Supplementary Figure 3L).

While MK2206 or BAY11-7085 effectively blocked PGE<sub>2</sub>-induced luciferase activity of a NF- $\kappa$ B response element, a  $\beta$ -catenin inhibitor, FH535, failed to do so (Figure 2L). Similarly, MK2206 or FH535 but not BAY11-7085 blocked PGE<sub>2</sub>-induced TOPflash activity (Figure 2M). Furthermore, MK2206, BEZ235, or BAY11-7085 but not FH535 inhibited the binding of NF- $\kappa$ B to the *MYC* promoter (Supplementary Figure 3M). Additive effects on expression of Myc (Supplementary Figure 3N) or MIR675-5p or H19 (Supplementary Figure 3O) was observed when both NF- $\kappa$ B and  $\beta$ -catenin were blocked.

### The tumor suppressor p53 is a direct target of MIR675-5p

To identify novel downstream targets of MIR675-5p in response to PGE<sub>2</sub> treatment, we used bioinformatics predictive approaches. RNAhybrid<sup>26</sup> analysis showed that there is a potential MIR675 binding site on the 3' untranslated region (UTR) of *TP53* mRNA with the minimum free energy of -31.7 kcal/mol (Supplementary Figure 4A). We employed RNA-ChIP assays to examine whether the *TP53* mRNA is selectively enriched in the Ago2/RISC complex after PGE<sub>2</sub> treatment or MIR675-5p overexpression. Indeed, PGE<sub>2</sub> treatment or MIR675-5p overexpression caused significant enrichment of *TP53* mRNA compared with

controls (Figure 3A). We also assessed several previously identified targets of MIR675-5p, including IGF1R, GPR55, MITF, RB, and CDC6, and found only increases of IGF1R and GPR55 mRNAs incorporated into RISC when MIR675-5p was overexpressed (Supplementary Figure 4B), confirming the previous notion that miRNAs suppress their targets in a context-dependent manner.

Further, we found that PGE<sub>2</sub> treatment caused downregulation of p53 and its direct target p21 in LS174T (Figure 3B) and SW48 (Supplementary Figure 4C) cells, both of which express wild-type p53 protein. CRISPR depletion of MIR675-5p not only increased the basal level of p53 but also blocked PGE<sub>2</sub>-induced downregulation of this protein. Re-expression of MIR675-5p (Supplementary Figure 4D) in depleted cells reversed this effect (Figure 3B and Supplementary Figure 4C). Overexpression of MIR675-5p reduced the expression of p53 and p21 (Figure 3C). In addition, upregulation of p53 and p21 expression caused by MIR675 depletion can be reversed by only MIR675-5p but not MIR675-3p rescue expression (Supplementary Figure 4E), suggesting MIR675-3p does not target p53. To further explore whether MIR675-5p directly suppresses p53 through the putative binding site in the 3'UTR of TP53 transcript, a luciferase reporter was obtained in which the full-length TP53 3'UTR (1207 bp)<sup>27</sup> with wild-type or mutated MIR675-5p binding site were embedded downstream of the firefly luciferase. First, PGE<sub>2</sub> treatment reduced luciferase expression of wild-type TP53 3'UTR, but did not affect expression of luciferase in tandem with the mutated TP53 3'UTR (Figure 3D). Moreover, a MIR675-5p inhibitor inhibited the effect of PGE<sub>2</sub> on reduction of TP53 promoter activity (Figure 3D). Secondly, the luciferase expression was elevated by the MIR675-5p inhibitor and repressed by MIR675-5p mimic, respectively (Figure 3 E and F). In contrast, neither MIR675-5p inhibitor nor mimic significantly altered the expression of the luciferase with mutated TP53 3'UTR (Figure 3 E and F). To further explore whether MIR675-5p and PGE<sub>2</sub> modulate the p53 signaling pathway, we employed a PCR array which profiles the expression of 84 genes related to p53-mediated signal transduction, including many direct targets of p53 such as p21. We first validated this array by comparing the expression of these genes in control and p53 CRISPR depletion LS174T cells. The expression of most genes including p21 was suppressed in p53 depletion cells compared with control cells (Supplementary Figure 4F). CRISPR depletion of MIR675 largely enhanced, whereas PGE<sub>2</sub> treatment reduced, the expression of these genes (Figure 3 G and H).

### **PGE<sub>2</sub> promotes CRC cell invasion and metastasis through MIR675-5p and p53**

To determine whether MIR675-5p is involved in PGE<sub>2</sub>-induced CRC cell migration/invasion and metastasis<sup>28-30</sup>, we first created three CRISPR constructs targeting different loci of MIR675 genomic sequence. All three sgRNAs effectively reduced the expression of MIR675-5p (Supplementary Figure 5A). Depletion of MIR675-5p strongly inhibited PGE<sub>2</sub>-induced cell invasion in both LS174T (Figure 4A) and SW48 (Supplementary Figure 5B) cells *in vitro*. Re-expression of MIR675-5p or CRISPR depletion of p53 in MIR675 CRISPR depletion cells reversed this effect (Figure 4B). Overexpression of wild-type p53 blocked PGE<sub>2</sub>-induced cell invasion (Figure 4C). These results reveal that PGE<sub>2</sub> enhances cell invasion through a MIR675-5p-p53 axis. Wild-type p53 negatively regulates cell migration and invasion<sup>31</sup>. Loss of p53 leads to increased levels of GTP bound (active)

RhoA and activated ROCK, its main effector protein. Most signals leading to altered cell migration and invasion converge on the Rho family of small GTPase<sup>32</sup> We found that a ROCK inhibitor Y27632 inhibited PGE<sub>2</sub>-induced cell invasion in LS174T (Figure 4D) and SW48 (Supplementary Figure 5C) cells, suggesting that RhoA is involved in PGE<sub>2</sub> promotion of cell invasion. Indeed, a pull-down assay revealed that PGE<sub>2</sub> treatment led to increased levels of GTP bound RhoA in LS174T (Figure 4E) and SW48 (Supplementary Figure 5D) cells. CRISPR depletion of MIR675-5p decreased level of GTP bound RhoA both in the presence and absence of PGE<sub>2</sub>. Re-expression of MIR675-5p or depletion of p53 in MIR675-5p depletion cells reversed this effect (Figure 4E and Supplementary Figure 5D). The activation of RhoA signaling by PGE<sub>2</sub> was further supported by increased phosphorylation of MYPT1, a substrate of ROCK, which also requires MIR675-5p (Figure 4F and Supplementary Figure 5E). Overexpression of p53 effectively blocked PGE<sub>2</sub>-induced RhoA activation (Figure 4G and Supplementary Figure 5F).

These *in vitro* results prompted us to explore whether MIR675-5p regulates CRC metastasis *in vivo*. We employed a CRC orthotopic model in which cells were injected into the cecal wall of NSG mice (Figure 5A). The mice were then treated with vehicle or PGE<sub>2</sub>. PGE<sub>2</sub> treatment increased the number of metastatic lesions both in the liver and lung (Figs. 5B, Supplementary Figure 6A). PGE<sub>2</sub> promotion of metastasis was not seen in mice carrying MIR675-5p depleted cells or wild-type p53 overexpressing (p53OE) cells (Figure 5B), demonstrating that the MIR675-5p-p53 pathway is required for PGE<sub>2</sub>-induced metastatic spread. The primary tumor weight in MIR675-5p depletion or p53OE group was slightly reduced compared to the control group (Supplementary Figure 6B). Tumor cells in the PGE<sub>2</sub> group displayed increased expression of MIR675-5p compared with the vehicle group (Supplementary Figure 6C), indicating that PGE<sub>2</sub> induced MIR675-5p *in vivo*. PGE<sub>2</sub> also reduced expression of p53 and p21 *in vivo* (Figure 5C). Similarly, we performed an independent experiment using anti-MIR675-5p (miRZip) sequences, these sequences inhibited the effect of PGE<sub>2</sub> on liver metastatic lesions (Supplementary Figure 6D). In support of these results, overexpression of MIR675-5p increased the number of liver metastatic lesions compared to control cells (Supplementary Figure 6E). Lastly, to demonstrate the crucial role of p53 in CRC metastasis, we injected cells with p53 CRISPR depletion. p53 depletion promoted liver and lung metastases to a level that was comparable to that of PGE<sub>2</sub> treatment (Figure 5D).

### **Expression of MIR675-5p and H19 correlates with that of COX-1 and COX-2 in CRC patients and predicts poor colorectal cancer patient survival**

To evaluate the clinical relevance of the expression of MIR675 and its precursor H19 to the prognosis of CRC patients, we analyzed multiple public datasets and found that high MIR675-5p (Figure 6 A and B) or H19 (Figure 6C) expression in CRC patients is associated with poorer disease-free survival and/or overall survival. Importantly, expression of PTGS1 (COX-1) or PTGS2 (COX-2) positively correlated with H19 expression (Figure 6D). Moreover, the protein expression of COX-2 was also positively correlated with that of MIR675-5p in a distinct tissue microarray cohort of CRC patients (Figure 6E). Interestingly, high H19 expression is associated with poorer overall survival in patients with high but not low COX-2 expression (Figure 6F). The smaller cohort of patients with available

MIR675-5p expression data reveal a similar association with survival (Supplementary Figure 7). In cultured CRC cells, inhibition of COX-2 by celecoxib, or by genetic COX-2 CRISPR depletion increased the expression of p53 and p21, which was reversed by PGE<sub>2</sub> treatment (Figure 6G and Supplementary Figure 8), consistent with the notion that COX-2 derived PGE<sub>2</sub> induces the expression of MIR675-5p which suppresses p53 expression.

## Discussion

There have been controversial reports as to whether the H19/MIR675 duo are pro-oncogenic or tumor-suppressive. Most studies have indicated that they are associated with growth, migration, invasion, and metastasis in many cancers; however, the reported functional mechanisms vary (reviewed in <sup>11</sup>). In CRC cells, H19 can function as a miRNA sponge to promote epithelial to mesenchymal transition and tumor growth <sup>33</sup> and MIR675 can increase cell growth via targeting the tumor suppressor gene, Rb <sup>16</sup> Their role in CRC invasion and metastasis has not been previously investigated. In a publicly available database of RNA-seq performed in matched normal colon, primary CRC, and metastatic CRC, the expression of Myc and H19 increase from normal colon epithelium to CRC primary tumors to metastatic tumors (Supplementary Figure 9). Our study establishes that PGE<sub>2</sub> can exert its biological functions, at least partially, through regulation of a miRNA. We identified MIR675-5p as a highly inducible miRNA that mediates the effect of PGE<sub>2</sub> on CRC invasion and metastasis by regulating the expression of tumor suppressor protein p53 and subsequent modulation of RhoA activity. Importantly, the expression of COX-1 and COX-2 correlated well with that of H19, the precursor of MIR675-5p, and with MIR675-5p expression, in CRC patients. High COX-2 expression in colorectal cancers, as well as elevated H19 or MIR675-5p expression predicts poor survival. Due to the unavailability of paired data for p53 protein expression levels and MIR675 or H19 expression, we were unable to analyze the correlation of p53 with MIR675-5p/H19 expression in CRC patients. This type of study is also complicated by the complex regulation of p53 protein expression including the effects of frequent mutations of this tumor suppressor protein in human cancer.

MiRNA expression in response to PGE<sub>2</sub> treatment has not previously been examined. We have identified more than 50 miRNAs whose expression might be altered significantly in response to a surge of PGE<sub>2</sub> in CRC cells. This sheds new light on our knowledge of the biological role of the pro-inflammatory bioactive lipid, PGE<sub>2</sub>. Interestingly, Hur *et al.* recently identified five miRNAs as potential markers of the development of liver metastases in CRC patients <sup>34</sup> Two of the downregulated miRNAs (miR-320, miR-221) in liver metastases identified in this study were also downregulated in PGE<sub>2</sub>-treated cells (Supplementary Table 1). Our study focused on MIR675-5p because it was most highly induced by PGE<sub>2</sub>. However, the significance of changes of other miRNAs identified here needs to be further evaluated and explored.

As an important inflammatory mediator, PGE<sub>2</sub> plays a critical role in guiding and governing various aspects of the inflammatory response in humans <sup>35</sup> Not surprisingly, another upregulated miRNA in our screen was miR-146a (Supplementary Figure S1), which can be induced by different pro-inflammatory stimuli <sup>36</sup> as well. As is the case with MIR675-5p upregulation, the induction of this miRNA by PGE<sub>2</sub> is likely mediated by activation of NF-

$\kappa$ B which is essential for the induction of miR-146a transcription as well<sup>37</sup> Besides protein regulatory factors, miRNAs have emerged as key regulators of inflammation, and it is likely that they modulate signaling of onset and termination of inflammation<sup>38,39</sup> Here we propose MIR675-5p is a new player in inflammatory responses. Its precise role in regulation of inflammation associated with other cancers is yet to be determined.

As a direct target of MIR675-5p, wild-type p53 may link PGE<sub>2</sub> with inflammation and cancer. A causative relationship between chronic inflammation and cancer is a well-accepted paradigm<sup>40</sup> However, the underlying mechanisms remain largely hypothetical. The link between chronic inflammation and cancer suggests that inflammation, largely controlled by NF- $\kappa$ B, must interfere with natural tumor suppressor mechanisms, of which wild-type p53 is extremely important. Hence, an obvious hypothesis is that the carcinogenicity of chronic inflammation is due to p53 suppression downstream of activated NF- $\kappa$ B. Indeed, this hypothesis is supported by findings from many studies (reviewed in<sup>41</sup>). A direct molecular link initiated from NF- $\kappa$ B to p53 has not been established. Our study shows that PGE<sub>2</sub>-activated NF- $\kappa$ B can promote transcription of the *Myc* oncogene, in turn, as a transcription factor, *Myc* drives the upregulation of H19, leading to increased expression of MIR675-5p, which represses the protein translation of wild-type p53 in CRC cells. This adds a new tier of regulation to the interaction between wild-type p53 and NF- $\kappa$ B. Other inflammatory mediators can regulate the expression of p53 as well. The pro-inflammatory cytokine Interleukin 6 downregulates p53 expression and activity by stimulating ribosome biogenesis in CRC cells<sup>42</sup> These results suggest the establishment of inflammation may create a situation in which p53 can no longer effectively exert its function as an eradicator of transformation-prone cells. Interestingly, a recent study demonstrated that MIR675 can directly target p53 that impacts apoptosis induced by brain injury in mice, corroborating our findings and expanding the role of MIR675<sup>43</sup>

*TP53* gene hemizygous deletion and point mutations frequently occur in CRC<sup>44</sup> The metastatic potential of tumor cells can be positively influenced by loss of wild-type p53 or expression of p53 gain-of-function mutants<sup>31</sup>. p53 directly influences transcription of genes involved in metastasis by binding promoters of a variety of genes known to be involved in regulating cell motility and adhesion, processes that are important for metastatic spread of disease<sup>45</sup>. Most signals leading to altered cell migration and invasion converge on the Rho family of small GTPases. Members of this family, including Rac, cdc42, and Rho, control actin dynamics and are integral to cytoskeletal changes accompanying tumor cell migration and invasion<sup>46,47</sup> Loss of p53 leads to increased levels of GTP-bound (active) RhoA and activated ROCK, its main effector protein<sup>48</sup> Overexpression and activation of RhoA is widely believed to contribute to the metastatic process in multiple tumor types<sup>49-53</sup> It has been shown that RhoA is overexpressed in CRC tumors<sup>54</sup> and RhoA silencing was reported to suppress the growth of colon cancer xenografts in immunodeficient mice<sup>55</sup> However, a group of researchers argue that RhoA inactivation can enhance Wnt signaling and promote colorectal cancer<sup>56</sup>. Although this study has not been independently confirmed, one cannot rule out the possibility of context-dependent regulation. Our study supports a positive role for RhoA in promoting CRC invasion and metastasis. We reveal a novel PGE<sub>2</sub>-initiated axis in which upregulation of MIR675-5p is capable of suppressing the expression of wild-type

p53, leading to activation of RhoA-ROCK pathway and consequently increased CRC cell invasion and metastasis to liver and lung.

It is possible that MIR675-5p is also capable of suppressing mutant p53 expression assuming their 3'UTR sequences are mutation free. A recent report demonstrated that multiple single nucleotide variants (SNVs) were present in the TP53 3'UTR in tumor specimens from 244 patients with diffuse large B-cell lymphoma 1. Most of the newly identified 3'UTR SNVs were located at sites that are complementary to seed sequences of miRNAs that are predicted or experimentally known to target TP53. Three SNVs disrupt the seed match between miR-125b and the TP53 3'UTR, thereby impeding suppression of p53 by this miRNA. Therefore, it is likely that mutant p53 may be protected from suppression by MIR675-5p due to the presence of SNVs. Interestingly, there is a SNV (G>A) that disrupts the seed match between MIR675-5p and the TP53 3'UTR (Supplementary Figure 10A) in patients with diffuse large B-cell lymphoma 1. This mutation effectively blocked the effect of MIR675-5p mimics or inhibitors on the TP53 3' UTR in a luciferase reporter assay (Supplementary Figure 10B). In agreement, we found that MIR675-5p is capable of targeting mutant p53 in DLD1 cells whose 3'UTR remains mutation free (confirmed by sequencing) in the seed sequence of MIR675-5p (Supplementary Figure 10C).

In conclusion, while targeting PGE<sub>2</sub> production remains a promising clinical direction in cancer therapy, finding a selective therapeutic window might be challenging due to its critical role in mucosal homeostasis and wound repair<sup>35</sup> Our findings provide a unique opportunity to target MIR675-5p, an important downstream effector of PGE<sub>2</sub> to inhibit CRC metastasis. It is less likely to cause cardiovascular toxicity because the levels of PGE<sub>2</sub> are not affected. The role of MIR675-5p in CRC metastasis is supported by the work reported here, but requires further study to assess its value in diagnostic, prognostic, or therapeutic clinical management. Given its role in promoting metastasis through p53 suppression, expression of MIR675-5p may have value as a prognostic biomarker to predict the metastatic potential of primary tumors. MiRNAs have also been used as diagnostic biomarkers circulating in the bloodstream. Further work is needed to test whether MIR675-5p is detectable in the bloodstream, as well as the specificity of its expression for advanced CRC. Our findings not only reveal a novel mechanism by which PGE<sub>2</sub> promotes CRC metastasis, but also provide a rationale to target MIR675-5p in CRC prevention and treatment.

## Supplementary Material

Refer to Web version on PubMed Central for supplementary material.

## Acknowledgments

**Grant Support:** This work is supported by NIH R01 DK047297, CA184820, and P01 CA077839 (to R.N.D.). The project described is also supported by the NIH National Center for Advancing Translational Sciences (NCATS) through Grant Number UL1 TR001450 (to B.C.).

## Abbreviations

**PG** Prostaglandins

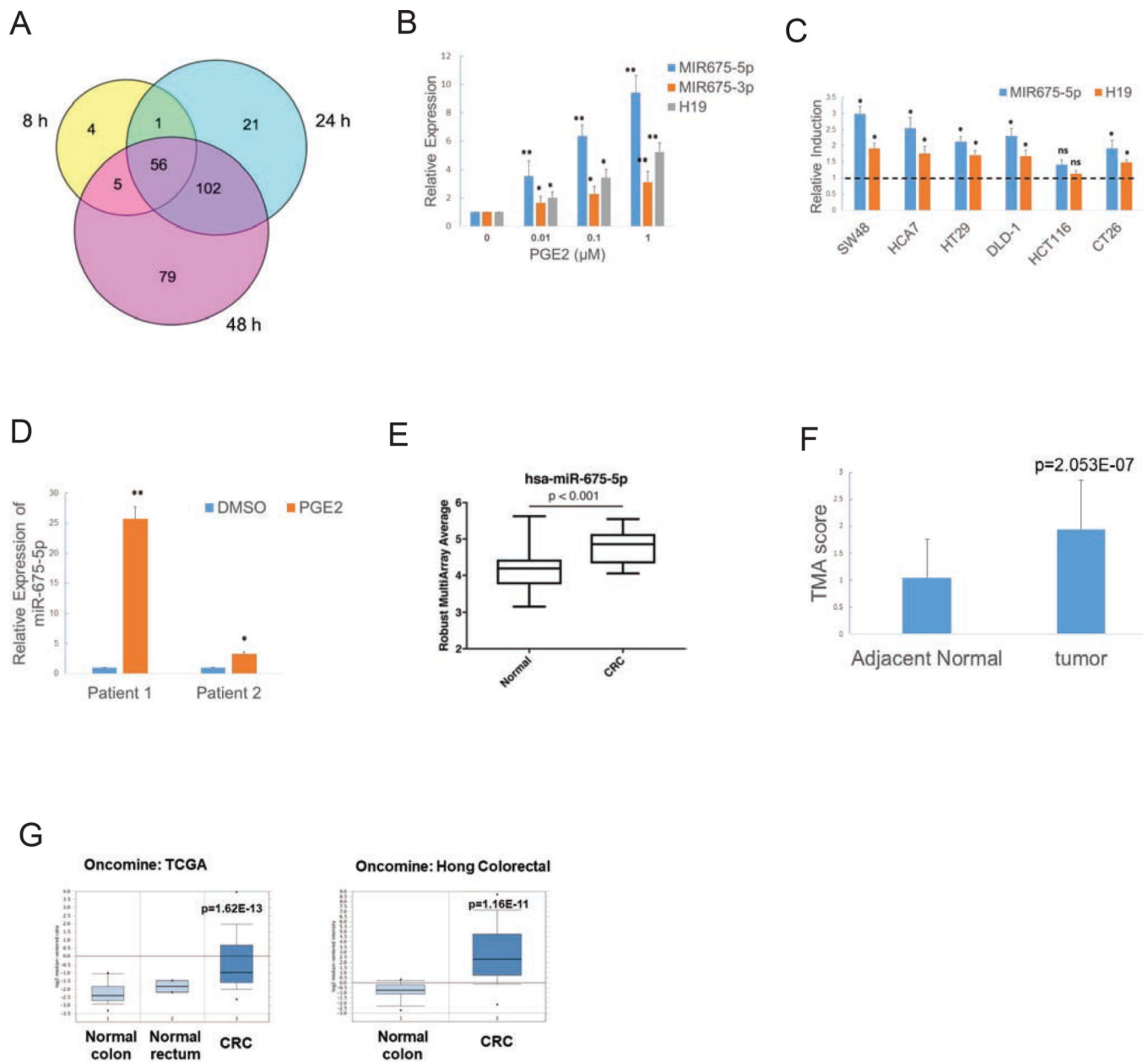
<b>CRC</b>	miRNA, microRNA; colorectal cancer
<b>UTR</b>	untranslated region
<b>ChIP</b>	chromosome immunoprecipitation
<b>OE</b>	over-expression
<b>qPCR</b>	quantitative polymerase chain reaction
<b>CRISPR</b>	clustered regularly interspaced short palindromic repeats

## References

1. Wang D, Dubois RN. Eicosanoids and cancer. *Nat Rev Cancer* 2010;10:181–93. [PubMed: 20168319]
2. Dubois RN, Abramson SB, Crofford L, et al. Cyclooxygenase in biology and disease. *FASEB J* 1998;12:1063–73. [PubMed: 9737710]
3. de Groot DJ, de Vries EG, Groen HJ, et al. Non-steroidal anti-inflammatory drugs to potentiate chemotherapy effects: from lab to clinic. *Crit Rev Oncol Hematol* 2007;61:52–69. [PubMed: 16945549]
4. Newcomb PA, Baron J, Cotterchio M, et al. Colon Cancer Family Registry: an international resource for studies of the genetic epidemiology of colon cancer. *Cancer Epidemiol Biomarkers Prev* 2007;16:2331–43. [PubMed: 17982118]
5. Ogino S, Kirkner GJ, Nosho K, et al. Cyclooxygenase-2 expression is an independent predictor of poor prognosis in colon cancer. *Clin Cancer Res* 2008;14:8221–7. [PubMed: 19088039]
6. Fischer SM, Hawk ET, Lubet RA. Coxibs and other nonsteroidal anti-inflammatory drugs in animal models of cancer chemoprevention. *Cancer Prev Res (Phila)* 2011;4:1728–35. [PubMed: 21778329]
7. McLemore TL, Hubbard WC, Litterst CL, et al. Profiles of prostaglandin biosynthesis in normal lung and tumor tissue from lung cancer patients. *Cancer Res* 1988;48:3140–7. [PubMed: 3130187]
8. Rigas B, Goldman IS, Levine L. Altered eicosanoid levels in human colon cancer. *J Lab Clin Med* 1993;122:518–23. [PubMed: 8228569]
9. Wang D, Dubois RN. Cyclooxygenase-2: a potential target in breast cancer. *Semin Oncol* 2004;31:64–73.
10. Wang D, DuBois RN. Urinary PGE-M: a promising cancer biomarker. *Cancer Prev Res (Phila)* 2013;6:507–10. [PubMed: 23636051]
11. Raveh E, Matouk IJ, Gilon M, et al. The H19 Long non-coding RNA in cancer initiation, progression and metastasis - a proposed unifying theory. *Mol Cancer* 2015;14:184. [PubMed: 26536864]
12. Cai X, Cullen BR. The imprinted H19 noncoding RNA is a primary microRNA precursor. *RNA* 2007;13:313–6. [PubMed: 17237358]
13. Keniry A, Oxley D, Monnier P, et al. The H19 lincRNA is a developmental reservoir of miR-675 that suppresses growth and Igf1r. *Nat Cell Biol* 2012;14:659–65. [PubMed: 22684254]
14. Shi Y, Wang Y, Luan W, et al. Long non-coding RNA H19 promotes glioma cell invasion by deriving miR-675. *PLoS One* 2014;9:e86295. [PubMed: 24466011]
15. Li H, Yu B, Li J, et al. Overexpression of lincRNA H19 enhances carcinogenesis and metastasis of gastric cancer. *Oncotarget* 2014;5:2318–29. [PubMed: 24810858]
16. Tsang WP, Ng EK, Ng SS, et al. Oncofetal H19-derived miR-675 regulates tumor suppressor RB in human colorectal cancer. *Carcinogenesis* 2010;31:350–8. [PubMed: 19926638]
17. He D, Wang J, Zhang C, et al. Down-regulation of miR-675-5p contributes to tumor progression and development by targeting pro-tumorigenic GPR55 in non-small cell lung cancer. *Mol Cancer* 2015;14:73. [PubMed: 25889562]
18. Yu YQ, Weng J, Li SQ, et al. MiR-675 Promotes the Growth of Hepatocellular Carcinoma Cells Through the Cdc25A Pathway. *Asian Pac J Cancer Prev* 2016;17:3881–5. [PubMed: 27644634]

19. Vennin C, Spruyt N, Dahmani F, et al. H19 non coding RNA-derived miR-675 enhances tumorigenesis and metastasis of breast cancer cells by downregulating c-Cbl and Cbl-b. *Oncotarget* 2015;6:29209–23. [PubMed: 26353930]
20. Zhou YW, Zhang H, Duan CJ, et al. miR-675-5p enhances tumorigenesis and metastasis of esophageal squamous cell carcinoma by targeting REPS2. *Oncotarget* 2016;7:30730–47. [PubMed: 27120794]
21. Zhu M, Chen Q, Liu X, et al. lncRNA H19/miR-675 axis represses prostate cancer metastasis by targeting TGFBI. *FEBS J* 2014;281:3766–75. [PubMed: 24988946]
22. Liu C, Chen Z, Fang J, et al. H19-derived miR-675 contributes to bladder cancer cell proliferation by regulating p53 activation. *Tumour Biol* 2016;37:263–70. [PubMed: 26198047]
23. Barsyte-Lovejoy D, Lau SK, Boutros PC, et al. The c-Myc oncogene directly induces the H19 noncoding RNA by allele-specific binding to potentiate tumorigenesis. *Cancer Res* 2006;66:5330–7. [PubMed: 16707459]
24. Bai D, Ueno L, Vogt PK. Akt-mediated regulation of NFkappaB and the essentialness of NFkappaB for the oncogenicity of PI3K and Akt. *Int J Cancer* 2009;125:2863–70. [PubMed: 19609947]
25. Castellone MD, Teramoto H, Williams BO, et al. Prostaglandin E2 promotes colon cancer cell growth through a Gs-axin-beta-catenin signaling axis. *Science* 2005;310:1504–10. [PubMed: 16293724]
26. Rehmsmeier M, Steffen P, Hochsmann M, et al. Fast and effective prediction of microRNA/target duplexes. *RNA* 2004;10:1507–17. [PubMed: 15383676]
27. Chen J, Kastan MB. 5'-3'-UTR interactions regulate p53 mRNA translation and provide a target for modulating p53 induction after DNA damage. *Genes Dev* 2010;24:2146–56. [PubMed: 20837656]
28. Buchanan FG, Wang D, Bargiacchi F, et al. Prostaglandin E2 regulates cell migration via the intracellular activation of the epidermal growth factor receptor. *J Biol Chem* 2003;278:35451–7. [PubMed: 12824187]
29. Kim JI, Lakshmikanthan V, Frilot N, et al. Prostaglandin E2 promotes lung cancer cell migration via EP4-betaArrestin1-c-Src signalsome. *Mol Cancer Res* 2010;8:569–77. [PubMed: 20353998]
30. Lu X, Han J, Xu X, et al. PGE2 Promotes the Migration of Mesenchymal Stem Cells through the Activation of FAK and ERK1/2 Pathway. *Stem Cells Int* 2017;2017:8178643. [PubMed: 28740516]
31. Powell E, Piwnica-Worms D, Piwnica-Worms H. Contribution of p53 to metastasis. *Cancer Discov* 2014;4:405–14. [PubMed: 24658082]
32. Muller PA, Vousden KH, Norman JC. p53 and its mutants in tumor cell migration and invasion. *J Cell Biol* 2011;192:209–18. [PubMed: 21263025]
33. Liang WC, Fu WM, Wong CW, et al. The lncRNA H19 promotes epithelial to mesenchymal transition by functioning as miRNA sponges in colorectal cancer. *Oncotarget* 2015;6:22513–25. [PubMed: 26068968]
34. Hur K, Toiyama Y, Schetter AJ, et al. Identification of a metastasis-specific MicroRNA signature in human colorectal cancer. *J Natl Cancer Inst* 2015;107.
35. Nakanishi M, Rosenberg DW. Multifaceted roles of PGE2 in inflammation and cancer. *Semin Immunopathol* 2013;35:123–37. [PubMed: 22996682]
36. Taganov KD, Boldin MP, Chang KJ, et al. NF-kappaB-dependent induction of microRNA miR-146, an inhibitor targeted to signaling proteins of innate immune responses. *Proc Natl Acad Sci U S A* 2006;103:12481–6. [PubMed: 16885212]
37. Larner-Svensson HM, Williams AE, Tsitsiou E, et al. Pharmacological studies of the mechanism and function of interleukin-1beta-induced miRNA-146a expression in primary human airway smooth muscle. *Respir Res* 2010;11:68. [PubMed: 20525168]
38. Tahamtan A, Teymooori-Rad M, Nakstad B, et al. Anti-Inflammatory MicroRNAs and Their Potential for Inflammatory Diseases Treatment. *Front Immunol* 2018;9:1377. [PubMed: 29988529]
39. O'Connell RM, Rao DS, Baltimore D. microRNA regulation of inflammatory responses. *Annu Rev Immunol* 2012;30:295–312. [PubMed: 22224773]

40. Gudkov AV, Gurova KV, Komarova EA. Inflammation and p53: A Tale of Two Stresses. *Genes Cancer* 2011;2:503–16. [PubMed: 21779518]
41. Gudkov AV, Komarova EA. p53 and the Carcinogenicity of Chronic Inflammation. *Cold Spring Harb Perspect Med* 2016;6.
42. Brighenti E, Calabrese C, Liguori G, et al. Interleukin 6 downregulates p53 expression and activity by stimulating ribosome biogenesis: a new pathway connecting inflammation to cancer. *Oncogene* 2014;33:4396–406. [PubMed: 24531714]
43. Yang S, Tang W, He Y, et al. Long non-coding RNA and microRNA-675/let-7a mediates the protective effect of melatonin against early brain injury after subarachnoid hemorrhage via targeting TP53 and neural growth factor. *Cell Death Dis* 2018;9:99. [PubMed: 29367587]
44. Baker SJ, Fearon ER, Nigro JM, et al. Chromosome 17 deletions and p53 gene mutations in colorectal carcinomas. *Science* 1989;244:217–21. [PubMed: 2649981]
45. Wei CL, Wu Q, Vega VB, et al. A global map of p53 transcription-factor binding sites in the human genome. *Cell* 2006;124:207–19. [PubMed: 16413492]
46. Bishop AL, Hall A. Rho GTPases and their effector proteins. *Biochem J* 2000;348 Pt 2:241–55. [PubMed: 10816416]
47. Heasman SJ, Ridley AJ. Mammalian Rho GTPases: new insights into their functions from in vivo studies. *Nat Rev Mol Cell Biol* 2008;9:690–701. [PubMed: 18719708]
48. Xia M, Land H. Tumor suppressor p53 restricts Ras stimulation of RhoA and cancer cell motility. *Nat Struct Mol Biol* 2007;14:215–23. [PubMed: 17310253]
49. Faried A, Nakajima M, Sohda M, et al. Correlation between RhoA overexpression and tumour progression in esophageal squamous cell carcinoma. *Eur J Surg Oncol* 2005;31:410–4. [PubMed: 15837049]
50. Kamai T, Kawakami S, Koga F, et al. RhoA is associated with invasion and lymph node metastasis in upper urinary tract cancer. *BJU Int* 2003;91:234–8. [PubMed: 12581011]
51. Chan CH, Lee SW, Li CF, et al. Deciphering the transcriptional complex critical for RhoA gene expression and cancer metastasis. *Nat Cell Biol* 2010;12:457–67. [PubMed: 20383141]
52. Horiuchi A, Imai T, Wang C, et al. Up-regulation of small GTPases, RhoA and RhoC, is associated with tumor progression in ovarian carcinoma. *Lab Invest* 2003;83:861–70. [PubMed: 12808121]
53. Mardilovich K, Olson MF, Baugh M. Targeting Rho GTPase signaling for cancer therapy. *Future Oncol* 2012;8:165–77. [PubMed: 22335581]
54. Fritz G, Just I, Kaina B. Rho GTPases are over-expressed in human tumors. *Int J Cancer* 1999;81:682–7. [PubMed: 10328216]
55. Wang H, Zhao G, Liu X, et al. Silencing of RhoA and RhoC expression by RNA interference suppresses human colorectal carcinoma growth in vivo. *J Exp Clin Cancer Res* 2010;29:123. [PubMed: 20828398]
56. Rodrigues P, Macaya I, Bazzocco S, et al. RHOA inactivation enhances Wnt signalling and promotes colorectal cancer. *Nat Commun* 2014;5:5458. [PubMed: 25413277]

**Figure 1.**

Identification of MIR675-5p as a top candidate induced by PGE<sub>2</sub> in CRC cells. (A) A Venn diagram representation of miR-Seq results showing the numbers of miRNAs significantly up- or down-regulated [False discovery rate (FDR) < 0.4] in LS174T cells treated with PGE<sub>2</sub> for 8, 24, and 48 h relative to control cells. (B) Expression of MIR675-5p, MIR675-3p, and H19 was examined by qPCR in LS174T cells. \**P* < .05, \*\**P* < .02, compared with no PGE<sub>2</sub> treatment. (C) Expression of MIR675-5p and H19 was examined by qPCR in CRC cell lines treated with 1 μM PGE<sub>2</sub> for 24 h. Results are relative to the respective cell line treated with DMSO. \**P* < .05, \*\**P* < .02; ns, not significant, compared with the DMSO treatment. (D) Expression of MIR675-5p was examined by qPCR in human CRC patient specimens treated with 1 μM PGE<sub>2</sub> for 24 h. \**P* < .05, compared with the DMSO treatment. (E) Expression of

MIR675-5p in tumor tissues of CRC patients (n=20) compared with normal tissues (n=20), as analyzed from published dataset GSE83924. (F) Expression of MIR675-5p in tumor tissues of CRC patients (n=50) compared with adjacent normal tissues (n=50) in a CRC tissue microarray revealed by *in situ* hybridization. (G) Expression of H19 in tumor tissues of CRC patients compared with normal tissues, as analyzed from published datasets TCGA (n=19, 3, and 101 for normal colon, normal rectum, and CRC, respectively) and Hong Colorectal Cancer (n=12 and 70 for normal colon and CRC, respectively). All data are presented as the mean  $\pm$  SD unless otherwise specified.

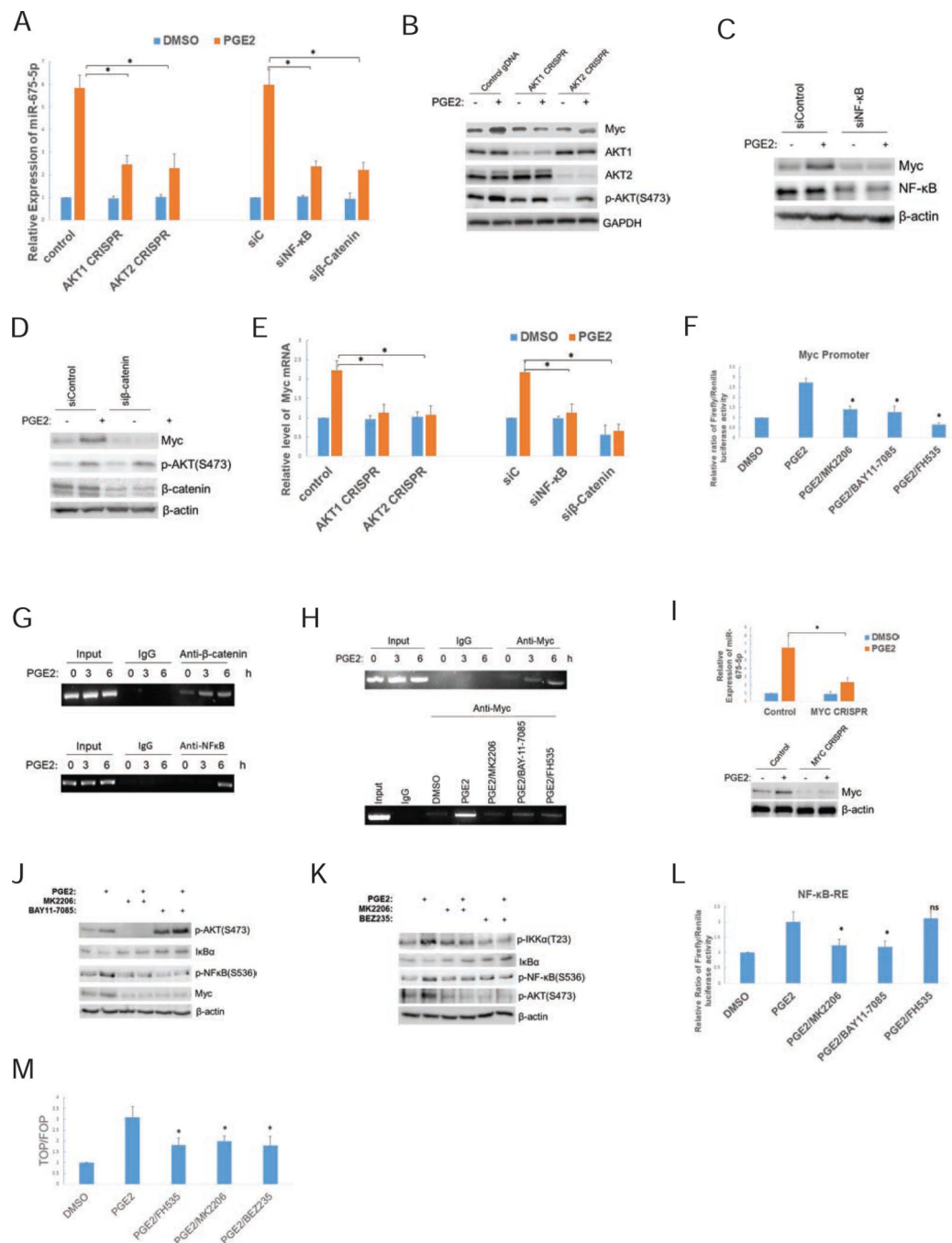


**Figure 2. NF-κB and β-catenin converge on Myc promoter to control MIR675-5p expression.** (A) Expression of MIR675-5p was examined by qPCR in LS174T cells with reduced AKT1 (CRISPR), AKT2 (CRISPR), NF-κB (siRNA), or β-catenin (siRNA) expression compared with control cells. Cells were treated with 1 μM PGE<sub>2</sub> or DMSO for 24 h. \*  $P < .05$ . (B) Protein expression was examined by Western analysis. Cells were treated with 1 μM PGE<sub>2</sub> or DMSO for 6 h. (C, D) Protein expression was examined by Western blot analyses. LS174T cells were transfected with siRNAs targeting NF-κB (C) or β-catenin (D) or a control siRNA prior to treatment with PGE<sub>2</sub> or DMSO for 8 h. (E) Expression of Myc

mRNA was examined by qPCR in cells indicated in (A). Cells were treated with 1  $\mu$ M PGE<sub>2</sub> or DMSO for 8 h. \*  $P < .05$ . (F) The activity of *Myc* promoter was examined by a dual-luciferase reporter assay in LS174T cells. Cells were treated with 1  $\mu$ M MK2206, 10  $\mu$ M BAY11-7085, or 10  $\mu$ M FH535 for 30 min before adding PGE<sub>2</sub> (1  $\mu$ M) for 8 h. \*  $P < .05$ , compared with the PGE<sub>2</sub> treatment. (G) The binding of  $\beta$ -catenin or NF- $\kappa$ B to the *Myc* promoter in response to PGE<sub>2</sub> treatment was examined by PCR following a ChIP assay. (H) The binding of *Myc* to the *H19* promoter in response to PGE<sub>2</sub> treatment (upper panel); or PGE<sub>2</sub> treatment in the absence or presence of inhibitors (lower panel) was examined by PCR following a ChIP assay. (I) Expression of MIR675-5p was examined by qPCR in cells with *Myc* CRISPR depletion. The effect of *Myc* depletion was demonstrated with Western analysis. Cells were treated with PGE<sub>2</sub> or DMSO. \*  $P < .05$ . (J, K) Protein expression was examined by Western analyses in LS174T cells. Cells were treated with inhibitors for 30 min before adding PGE<sub>2</sub>. (L, M) The activity of NF- $\kappa$ B or  $\beta$ -catenin was examined by a luciferase reporter containing repeated NF- $\kappa$ B responsive element (L) or TCF binding sites (M). Cells were treated with inhibitors for 30 min before PGE<sub>2</sub> was added. \*  $P < .05$ ; ns, not significant, compared with the PGE<sub>2</sub> treatment. All data are presented as the mean  $\pm$  SD.

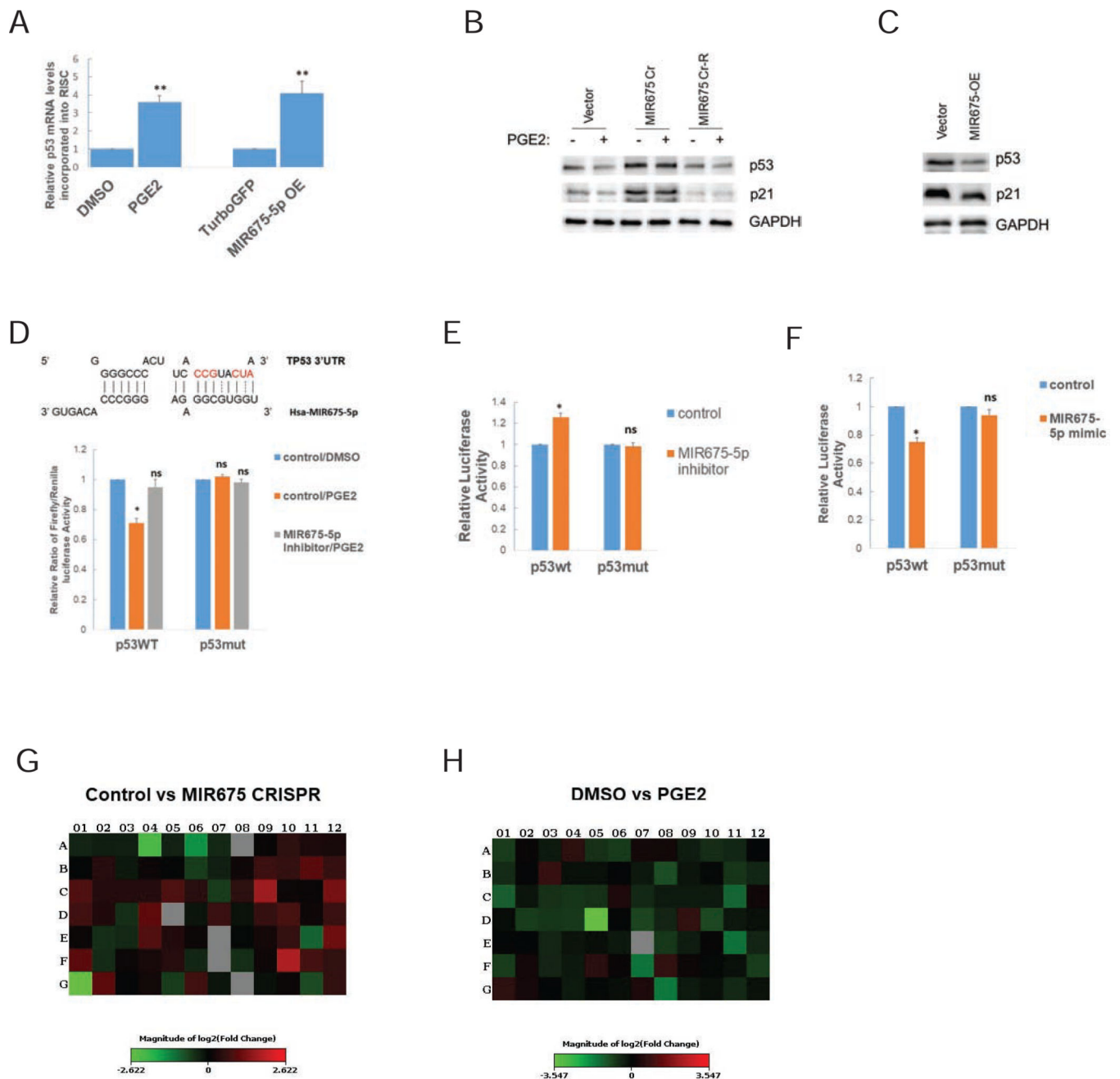


**Figure 3. Identification of p53 as a direct target of MIR675-5p.**

(A) RNA-ChIP analysis was conducted to detect levels of *TP53* mRNA that were incorporated into the Ago2-RISC complex from LS174T cells treated with or without PGE<sub>2</sub> or cells expressing indicated plasmids. \*\*  $P < .02$ . (B) Protein expression was examined by Western analysis in LS174T cells with indicated modifications: MIR675 Cr-R, MIR675-5p was re-expressed in cells with MIR675 CRISPR (Cr) depletion. (C) Protein expression was examined by Western analyses in LS174T cells with indicated modifications: MIR675-OE, MIR675 overexpression. (D) Alignment of MIR675-5p and its binding site in the 3'UTR of *TP53*. The nucleotides in the 3'UTR that were replaced to make the *TP53* mutant are

marked in red. Luciferase activity of the reporter construct containing the wild-type or MIR675-5p-binding mutant 3'UTR of *TP53* was measured after transfection with or without a MIR675-5p inhibitor into LS174T cells, which were treated with PGE<sub>2</sub> or DMSO. \*  $P < .05$ ; ns, not significant. (E, F) Luciferase activity of the reporter constructs in (D) was measured after transfection with or without a MIR675-5p inhibitor (E) or MIR675-5p mimic (F). \*  $P < .05$ . (G) MRNA levels of p53-regulated genes embedded in a PCR array in MIR675 CRISPR depletion cells relative to control cells were measured by qPCR. (H) The PCR array in (G) was used to measure mRNA levels of p53-regulated genes in PGE<sub>2</sub> treated cells relative to DMSO treated cells. All data are presented as the mean  $\pm$  SD.

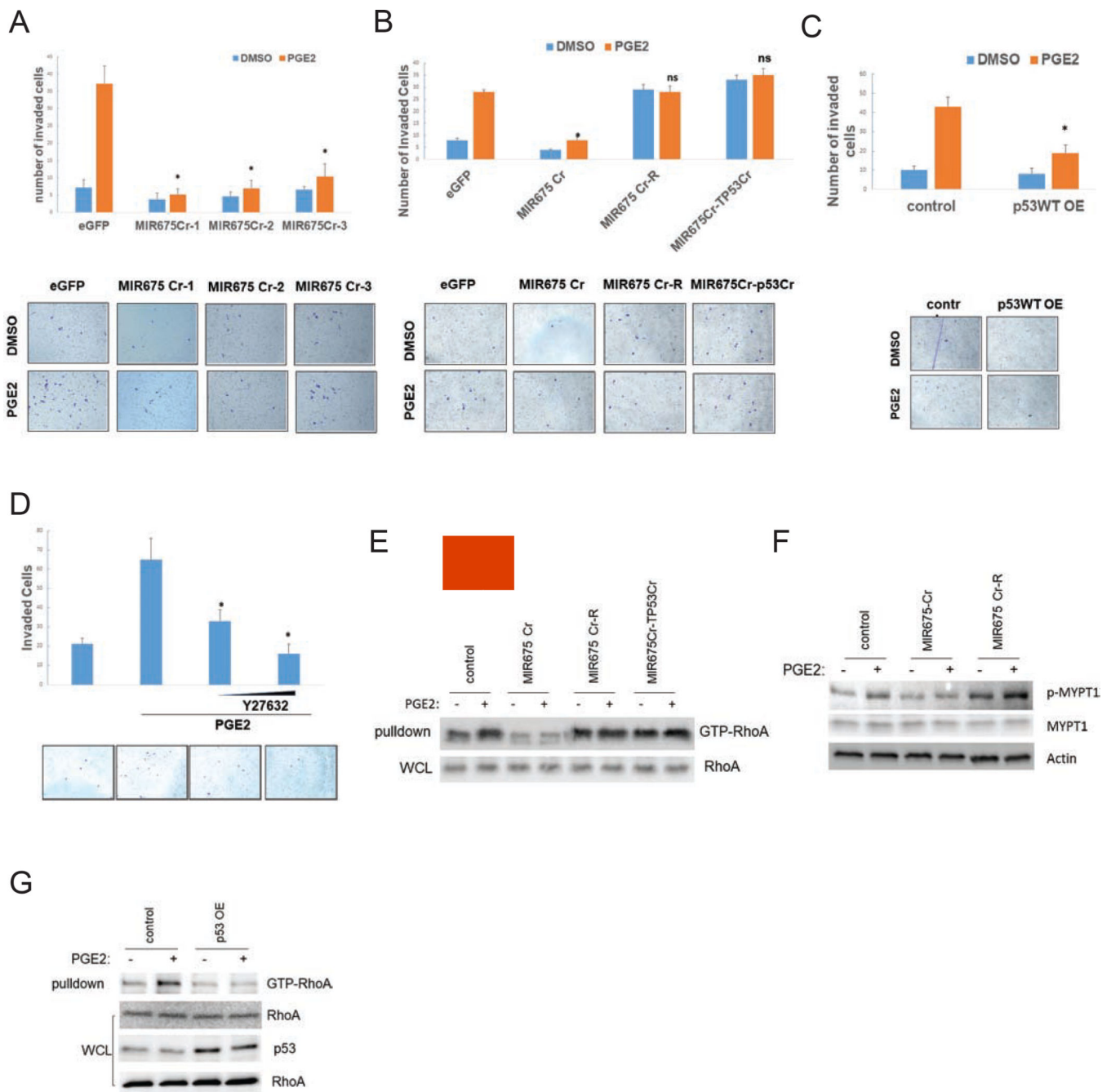


**Figure 4. MIR675-5p mediates PGE<sub>2</sub>-induced cell invasion through suppressing p53 expression and activation of RhoA signaling.**

(A) *In vitro* invasion of LS174T cells. Cells carrying a control construct or CRISPR (Cr) constructs targeting different loci in the MIR675 genomic sequence were treated with PGE<sub>2</sub> or DMSO. \*  $P < .05$ , compared with the eGFP treated with PGE<sub>2</sub>. (B) Invasion of LS174T cells carrying indicated constructs was measured as in (A). \*  $P < .05$ ; ns, not significant, compared with the eGFP treated with PGE<sub>2</sub>. (C) Effect of wild-type (WT) p53 overexpression (OE) on cell invasion of LS174T cells. \*  $P < .05$ , compared with the control treated with PGE<sub>2</sub>. (D) PGE<sub>2</sub>-induced cell invasion of LS174T cells was evaluated with or

without Y27632. \*  $P < .05$ , compared with the treatment with PGE<sub>2</sub> alone. (E) Activation of RhoA in LS174T cells. Cells carrying indicated constructs were treated with PGE<sub>2</sub> or DMSO. (F) Phosphorylation of MYPT1 was examined by Western analysis. LS174T cells were treated with PGE<sub>2</sub> or DMSO. (G) Levels of RhoA-GTP and expression of indicated protein in whole cell lysates (WCL) of LS174T cells were detected by Western analysis. All data are presented as the mean  $\pm$  SD.

Author Manuscript

Author Manuscript

Author Manuscript

Author Manuscript

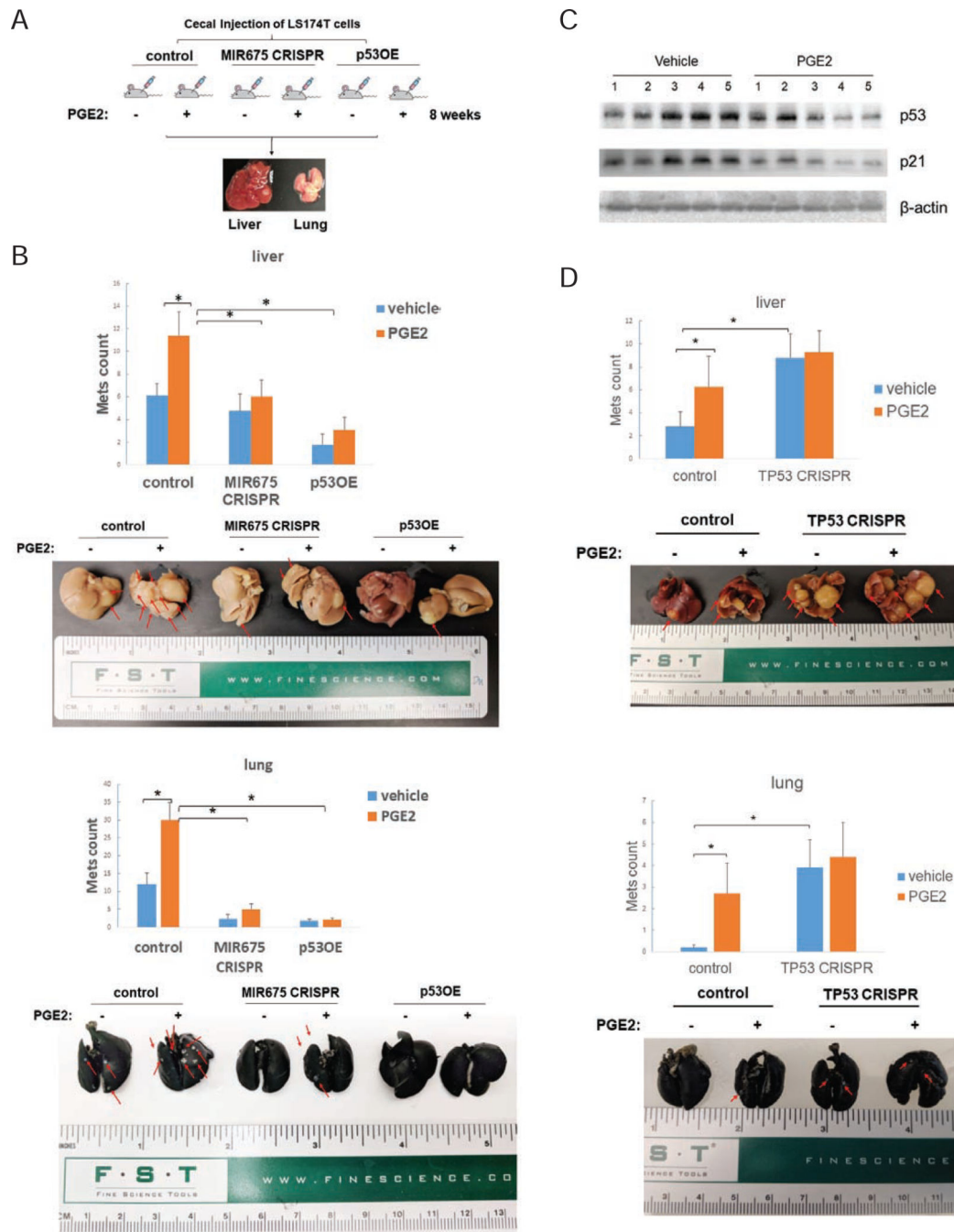


**Figure 5. MIR675 mediates PGE<sub>2</sub>-induced liver and lung metastases of CRC cells *in vivo*.**

(A) Schematic description of the metastatic model of CRC. (B) Mice carrying indicated cells (n=6) were treated with PGE<sub>2</sub> or vehicle. Tumor nodules on liver and lung were counted separately. Representative images of liver or lung with metastatic nodules are shown. Data are presented as the mean ± SEM (\**P* < .05). (C) Protein expression in primary cecal tumors from control cells treated with PGE<sub>2</sub> or vehicle was examined by Western analysis. (D) Mice carrying indicated cells (n=6) were treated with PGE<sub>2</sub> or vehicle. Tumor nodules on liver

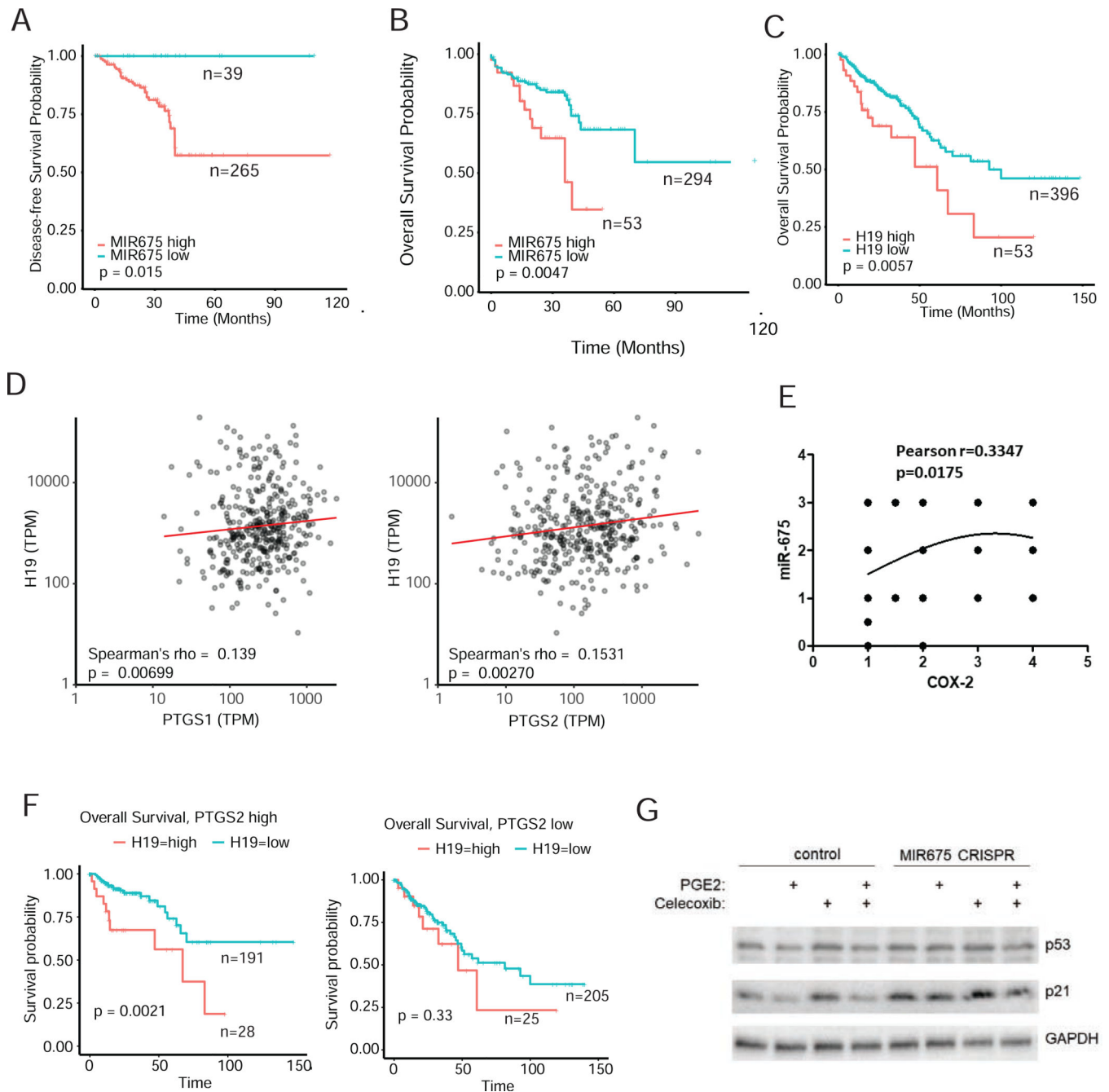
and lung were counted separately. Representative images of liver or lung with metastatic nodules are shown. Data are presented as the mean  $\pm$  SEM (\* $P < .05$ ).

Author Manuscript

Author Manuscript

Author Manuscript

Author Manuscript

**Figure 6.**

Clinical correlation of COXs-H19-MIR675-5p expression profiles and prognosis of CRC patients. Kaplan-Meier analysis of the TCGA CRC provisional dataset (2016 version) revealed that patients with high MIR675 (A-B) and H19 (C) expression demonstrate poorer disease-free survival (A) and overall survival (B-C). (D) Expression of COX-1 RNA (PTGS1) and COX-2 RNA (PTGS2) correlate with H19 expression in the TCGA CRC dataset. (E) Expression of MIR675 correlates with COX-2 expression as revealed by a CRC tissue microarray (n=50). (F) High H19 expression is associated with poorer overall survival in patients with high but not low COX-2 expression in the TCGA dataset. (G) Protein

expression was examined by Western analysis in LS174T cells with reduced expression of COX-2 or MIR675 achieved by CRISPR depletion or control cells. Cells were treated with PGE<sub>2</sub> or Celecoxib.

Author Manuscript

Author Manuscript

Author Manuscript

Author Manuscript